Quaternary Research 77 (2012) 12–22

Contents lists available at SciVerse ScienceDirect

Quaternary Research

journal homepage: www.elsevier.com/locate/yqres

Frequency and intensity of high-altitude floods over the last 3.5 ka in northwestern French Alps (Lake Anterne)

Charline Giguet-Covex [a,*], Fabien Arnaud [a], Dirk Enters [a,f], Jérôme Poulenard [b], Laurent Millet [c], Pierre Francus [d,e], Fernand David [g], Pierre-Jérôme Rey [a], Bruno Wilhelm [a], Jean-Jacques Delannoy [a]

[a] EDYTEM, Université de Savoie, CNRS Pôle Montagne, 73376 Le Bourget du Lac, France
[b] CARRTEL, INRA, Université de Savoie, Campus universitaire, 73376 Le Bourget du Lac, France
[c] Laboratoire de Chrono-Environnement, UMR 6249 CNRS, UFR Sciences et Techniques, Université de Franche-Comté, 25030 Besançon cedex, France
[d] Institut national de la recherche scientifique, Centre Eau, Terre et Environnment, Québec (Qc), Canada G1K 9A9
[e] GEOTOP, Geochemistry and Geodynamics Research Center, CP 8888, Montréal, QC, Canada H3C 3P8
[f] GEOPOLAR, Institute of Geography, University of Bremen, Germany
[g] Aix-Marseille Univ, CEREGE, UMR 6635, 13545 Aix en Provence cedex 4, France

ARTICLE INFO

Article history:
Received 14 April 2010
Available online 3 December 2011

Keywords:
Grain size
Itrax core scanner
Flood frequency
Extreme precipitation events
Climatic changes
Land use

ABSTRACT

In central Western Europe, several studies have shown that colder Holocene periods, such as the Little Ice Age, also correspond to wet periods. However, in mountain areas which are highly sensitive to erosion processes and where precipitation events can be localized, past evolution of hydrological activity might be more complicated. To assess these past hydrological changes, a paleolimnological approach was applied on a 13.4-m-long sediment core taken in alpine Lake Anterne (2063 m asl) and representing the last 3.5 ka. Lake sedimentation is mainly composed of flood deposits triggered by precipitation events. Sedimentological and geochemical analyses show that floods were more frequent during cold periods while high-intensity flood events occurred preferentially during warmer periods. In mild temperature conditions, both flood patterns are present. This underlines the complex relationship between flood hazards and climatic change in mountain areas. During the warmer and/or dryer times of the end of Iron Age and the Roman Period, both the frequency and intensity of floods increased. This is interpreted as an effect of human-induced clearing for grazing activities and reveals that anthropogenic interferences must be taken into account when reconstructing climatic signals from natural archives.

Introduction

Results of observational and modeling studies show, in the context of global warming, an increase of intense precipitation events in many regions of the globe (Easterling et al., 2000; Palmer and Räisänen, 2002). Theoretically, the rise of greenhouse gases would increase precipitation events of high intensity due to a change in the atmospheric moisture transport capacity (Trenberth, 1999; Allen and Ingram, 2002). In mountain areas, torrential floods are relatively frequent and cause considerable damages. Furthermore, these areas are particularly sensitive to climatic changes as shown by the comparison of mean temperature at high-elevation sites and at global scale (Beniston et al., 1997). The question of global warming effects on flood activity in mountains appears thus as an important issue. Since the 1980s an increase in the frequency of extreme precipitation events has been observed in the European Alps (Beniston et al., 1997; Rebetez et al., 1997). However, the lack of studies covering long time periods precludes such an evolution to be attributed to global warming. Furthermore, it is difficult to simulate extreme precipitations with GCMs and RCMs (General and Regional Circulation Models), because of the complexity of the topography in mountain areas. In particular, uncertainties of scenarios increase for summer precipitation of high intensity (Frei et al., 2003; 2006). Therefore, historical and natural archives represent interesting sources of information to better understand past and future evolution of flood and precipitation events (Rico et al., 2001; Benito et al., 2004; Schulte et al., 2009; Bussmann and Anselmetti, 2010).

Lakes are widely spread over mountain landscapes and act as natural traps of catchment erosion products. Therefore, the occurrence of erosive events such as torrential floods may be recorded in the stratigraphy of alpine lake sediments over long time periods (Leeman and Niessen, 1994; Nesje et al., 2001; Bøe et al., 2006). However, the climatic interpretation of changes in flood deposit frequency and thickness is not always straightforward. In particular, most European areas have encountered periods of human occupation, which affected vegetation, soil stability and thus the relationship between climate and erosion processes (Lanci et al., 2001; Dapples et al., 2002; Schmidt et al., 2002).

* Corresponding author.
E-mail address: charline.giguet-covex@univ-savoie.fr (C. Giguet-Covex).

0033-5894/$ – see front matter © 2011 University of Washington. Published by Elsevier Inc. All rights reserved.
doi:10.1016/j.yqres.2011.11.003

In a previous study covering the entire Holocene (Giguet-Covex et al., 2011), we showed that the Lake Anterne catchment became highly sensitive to climate-triggered changes in erosion patterns since 3.4 ka. We argued this was due to the intensive use of alpine mid-altitude area for grazing since the Bronze Age. Our current study aims at distinguishing detrital deposits linked to "normal precipitation" and/or snowmelt and the ones triggered by extreme heavy rainfall events, focussing on the last 3.5 ka in the light of a chironomid-inferred July air-temperature reconstruction (Millet et al., 2009) from the same lake sediment sequence. As the mobilization and transport of coarse sediments toward lakes reflect an increase of stream velocity and discharge (Campbell, 1998; Francus et al., 2002; Bøe et al., 2006; Parris et al., 2009), we used grain size as an indicator of paleoflood intensity. In order to have a high-resolution continuous record of flood intensity, a proxy of coarse particles was determined from geochemical measurement obtained with a core scanner. Relationships between flood frequency and intensity, land-use history and climate are also examined by comparison with other archives of climate and anthropogenic activities.

Study site and setting

Lake Anterne is a small alpine lake (0.12 km^2) located at 2063 m asl in the northern French Alps (Figs. 1A and B). Its catchment (2.55 km^2) is currently covered by meadow vegetation except in the south and east, which are characterized by steep slopes mainly formed by easily erodible rocks (calc schists and black shales). The lake is frozen during 6 to 7 months each year (recently, from ~11/23/2007 to 06/26/2008, from ~11/14/2008 to 06/05/2009, and from 12/02/2009 to ~06/20/2010 based on data from daily catchment pictures) and the southern slopes are rarely snow-free before July. Therefore, lake sediments only record erosion fluxes related to precipitation events occurring from early summer to mid-autumn. The absence of terrestrial debris fans shows that debris flows are not an important geomorphologic process in the catchment (Fig. 1C). However, debris-flow events cannot be totally excluded for the past.

Material and methods

The composite core, ANT-07, was retrieved in the deepest part of the lake in 2007 (Fig. 1D). In the present study we focus on this time period, corresponding to the uppermost 13.4 m of core ANT-07 (Fig. 2A). This core was correlated to core ANT-01 taken in 2001 (Arnaud et al., 2006; Millet et al., 2009) using lithological descriptions and in particular thick flood and gravity-reworked sediment deposits, as previously described by Arnaud et al. (2002). It was hence possible to compare Chironomid-inferred July air temperatures (Millet et al.,

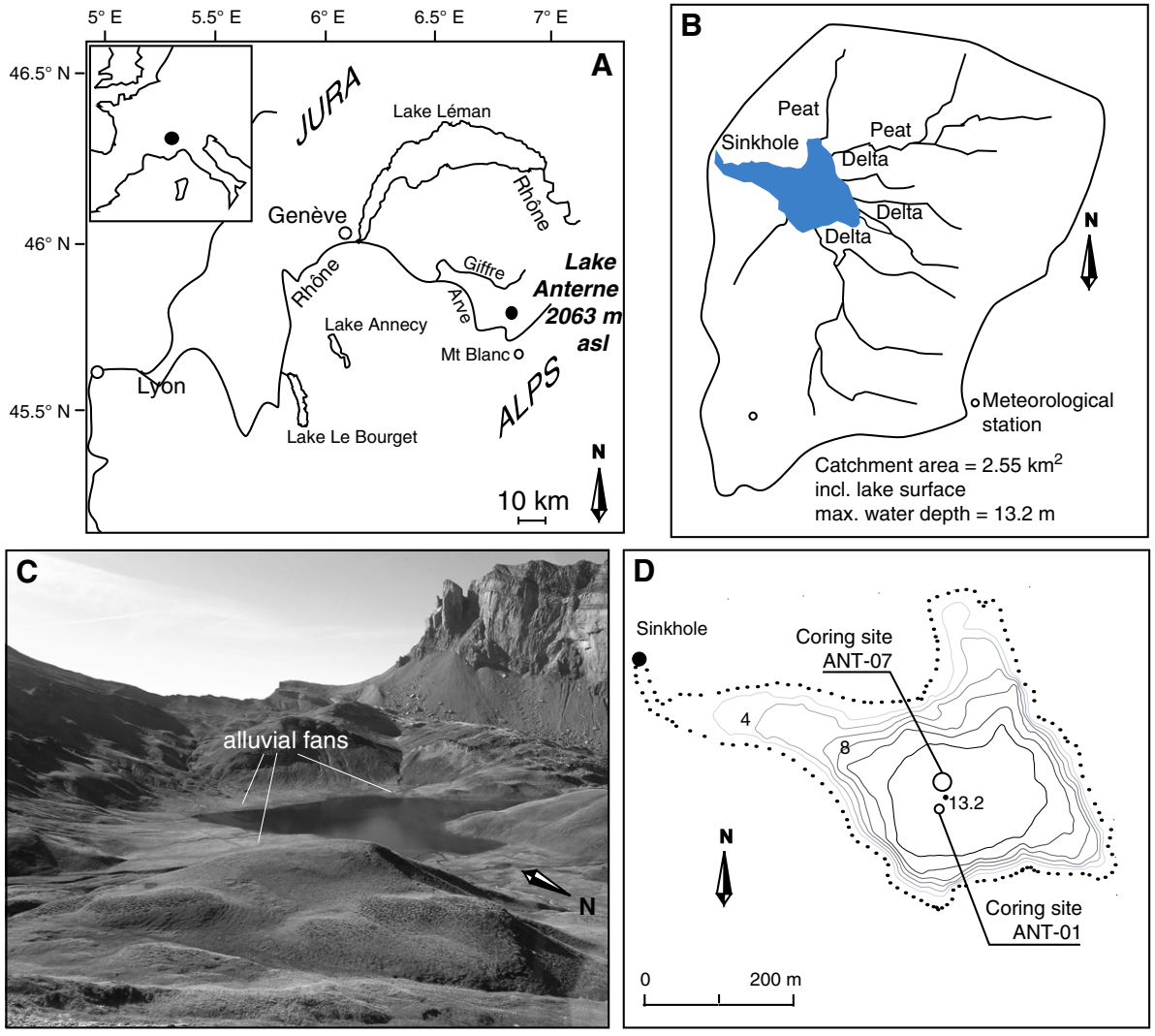

Figure 1. Overview maps of the geographical setting (A). Panels B and D present the catchment area with the water system and the bathymetric map with coring sites, respectively. Picture C illustrates the sediment transport processes in the Lake Anterne catchment. The presence of alluvial fans shows that sediments are mainly transferred during flood events.

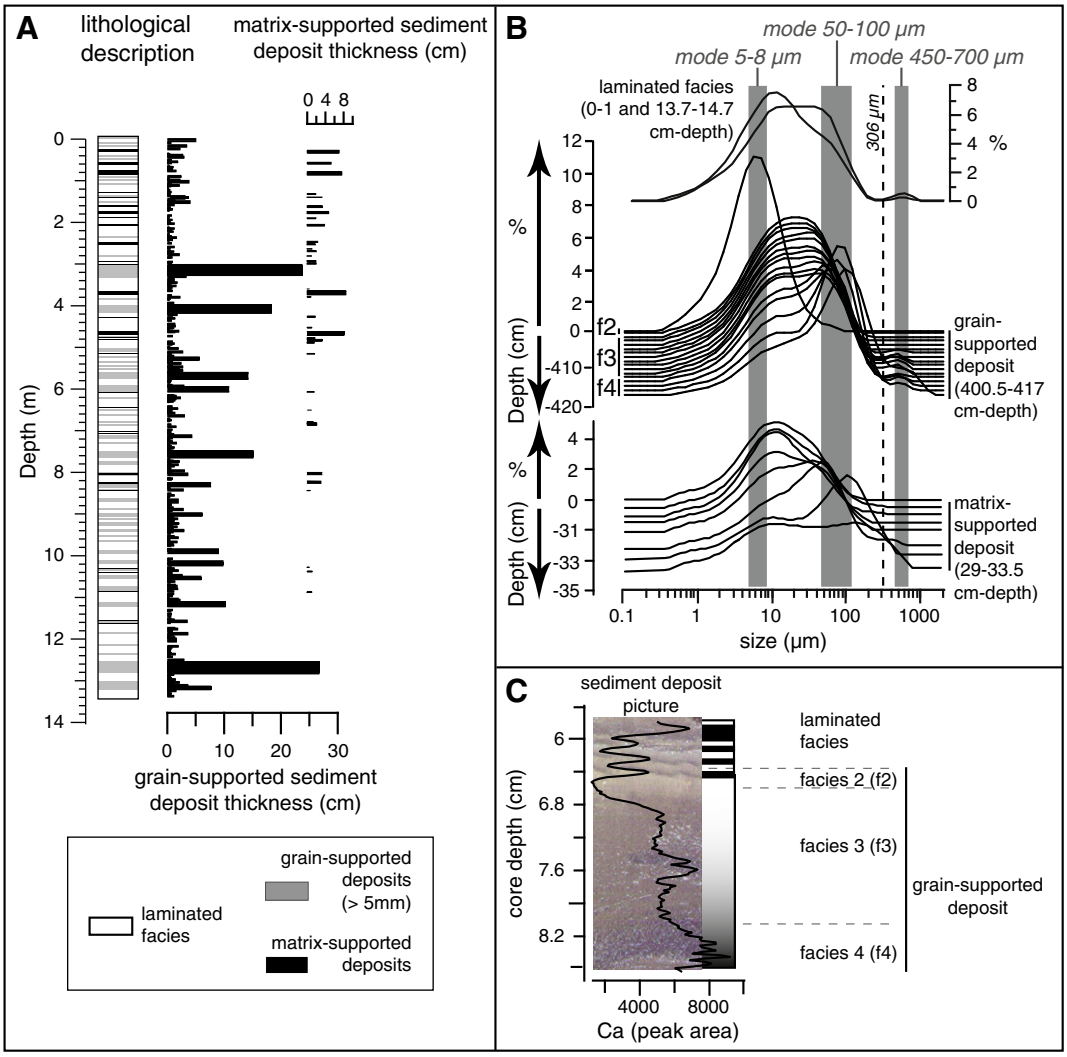

Figure 2. (A) Deposit thicknesses of lake sediment-core lithological units representing grain-supported sediments (flood deposits) and matrix-supported sediments (gravity-reworked sediment deposits). Grain-size distributions of laminated sediments and grain-supported and matrix-supported sequences are shown in B. A detailed lithological description and the calcium content of laminated sediments measured by XRF and grain-supported deposits are presented in C.

2009) obtained from core ANT-01 with the flood-intensity record presented in this study.

Flood deposits (thicker than 5 mm, i.e. visually recognizable) as described by Arnaud and others (2002) were visually identified and documented in terms of stratigraphic location and thickness. Flood deposit frequency was then computed as a running sum over a 100-yr time window as estimated by our age–depth model (see below). These thick flood deposits are intercalated with finer laminae couplets (dark and light layers) that were also counted for the first 10 m of the core. The frequency of these couplets was also determined using a running sum over a 10-yr time window.

Grain-size measurements were performed by laser diffraction using a Malvern Mastersizer 2000G covering a theoretical range from 0 to 2000 µm. A discontinuous sampling step strategy (between 1 and 30 cm) was applied in laminated sediments due to the occurrence of thick instantaneous deposits. Each sample integrates 1-cm sediment depth. In addition, grain-size measurements were performed on the coarse basal layer of each flood deposits thicker than 5 mm. The sorting index was calculated with the statistical equation developed by Trask (1930): $(P_{75}/P_{25})^{1/2}$.

High-resolution calcium analyses were conducted following a sampling step of 100 µm on the uppermost 10 m of core ANT-07 and of 200 µm between 10 and 13.4 m. These high-resolution XRF analyses were performed only on laminated sections (<5 mm), using an ITRAX core scanner (30 kV, 35 mA, 10 s sampling time) (Croudace et al., 2006). XRF measurements were resampled to build a data set with a single chemical value for each year and were then smoothed with a running mean over a 10-yr interval.

The age–depth model relies on twenty ^{14}C AMS measurements performed on terrestrial macroremains, of which four come from core ANT-01 and were stratigraphically correlated to the ANT-07 sediment core (Fig. 1C, Table 1). The age–depth model was then constructed by fitting a smooth spline curve using the "CLAM" program (Blaauw, 2010) developed under the mathematics software "R" version 2.12.2 (R Development Core Team, 2011). The used calibration curve was Intcal09 (Reimer et al., 2009). Lead pollution was also integrated to improve our age–depth model. Lead concentrations were measured at the Activation Laboratories (Ancaster, Ontario, Canada) using the Ultratrace protocol (near total digestion with HF, $HClO_4$, HNO_3 and HCl followed by ICP-MS measurements). The anthropogenic lead flux was then calculated using the method described by Arnaud et al. (2004) and considering a natural background of 19 ppm, which corresponds to average concentration of the pre-anthropogenic period between 2000 and 3500 cal yr BP.

Table 1
List of radiocarbon ages. Stars correspond to dates taken from the core ANT-01 and bold dates were removed before constructing the age–depth model.

Sample name	Laboratory	Cumulated depth (cm)	Depth (cm) (without events)	Sample type	Lithology	Radiocarbon age	Age cal yr BP 2 σ range
ANT 07 B1	POZ 25944	46	20.2	Tree bark	A-type seq.	190 ± 30	150 ± 150
ANT 07 B1b	POZ 30276	80.8	38.2	Wood and leaf	A-type seq.	170 ± 25	145 ± 145
ANT 01 01A*	GIFa 101287	208.5	102.8		A-type seq.	430 ± 80	470 ± 160
ANT 07 B2	GIFa 12209	269.6	142.9	Leaf	A-type seq.	395 ± 30	420 ± 95
ANT 01 02 A2*	GIFa 101288	327.5	163.1		A-type seq.	2410 ± 35	**2520 ± 180**
ANT 01 02 A2*	POZ 794	329	164.6		A-type seq.	640 ± 60	610 ± 70
ANT 07 C2	GIFa 12210	415.3	206.1	Leaf	A-type seq.	885 ± 30	820 ± 90
ANT 07 B3b	POZ 30277	536	265.1	Twig and leaf	A-type seq.	1300 ± 30	1235 ± 60
ANT 01 02 A2*	POZ 720	608.7	293.5		A-type seq.	1680 ± 35	1610 ± 90
ANT 07 C3	GIF12211	714.7	358.6	Tree bark	A-type seq.	4005 ± 30	**5170 ± 125**
ANT 07 B5b	POZ 30278	883.3	444.5	Plant macrofossils	A-type seq.	2650 ± 35	**2790 ± 55**
ANT 07 C4b	POZ 25946	905.8	451.4	Conifer shell	A-type seq.	2055 ± 35	2025 ± 95
ANT 07 B5b	POZ 30279	960.8	477.8	Wood	A-type seq.	2295 ± 35	2260 ± 100
ANT 07 B5b	GIF 10729	1009.1	504.3	Wood	A-type seq.	1690 ± 30	**1610 ± 80**
ANT 07 C5b	POZ 30280	1088.5	541.9	Charcoal	A-type seq.	2565 ± 30	2630 ± 125
ANT 07 B6b	POZ 25945	1123.8	555.6	Wood—Alnus/Corylus	A-type seq.	2620 ± 35	2730 ± 110
ANT 07 C6b	GIF 10726	1222.1	624	Wood	A-type seq.	2910 ± 20	3055 ± 90
ANT 07 C6b	POZ 30282	1294.3	655.3	Leaf and tree bark	A-type seq.	3100 ± 30	3320 ± 70
ANT 07 B7b	GIF 12212	1369.2	698	Wood and leafs	A-type seq.	3390 ± 30	3635 ± 70
ANT 07 C7b	POZ 30283	1403.75	720.6	Charcoal	L-type seq.	3795 ± 35	4180 ± 170
RSLA 1 niv. 2	POZ 33446	Archaeological site		Charcoal (*Pinus* sp.)		1835 ± 30	1785 ± 80
RSLA 1 niv.5b	SacA 20689	Archaeological site		Charcoal (conifer shell)		2230 ± 30	2245 ± 90

Results

Lithology

As described in previous papers (Arnaud et al., 2002; Giguet-Covex et al., 2011), the sediment record consists of two types of fining-upward deposits thicker than 5 mm that are interbedded in a rhythmic sedimentation made of couplets thinner than 5 mm.

Matrix-supported sediment deposits

The first type of fining-upward deposits are *matrix-supported* and contain coarse and poorly sorted sediments at their base as shown by grain-size distributions characterized by sorting values between 2.4 and 3.8 (Fig. 2B; Arnaud et al., 2002). Most of matrix-supported deposits (31 / 35) are located between 0 and 850 cm depth. Their thicknesses vary between 0.6 and 8.5 cm (Fig. 2A). Particle-size distributions (PSD) present two modes, one around 8–10 μm and another around 50–100 μm.

Grain-supported sediment deposits

The other fining-upward deposits are made of a succession of three facies (f4, f3, f2 from bottom to top): f4 = coarse, well-sorted sediments (sorting values between 1.95 and 3.06), f3 = mixture of silts and fine sands, and f2 = fine silts and clays (Figs. 2B and C). There is no sharp limit between f3 and f2. This type of deposit is described as *grain-supported* as there are few fine particles embedding the coarse fraction (f4) (Arnaud et al., 2002). This last feature, together with the presence of the whitish clay cap (f2 facies) is the criteria used to distinguish these types of sequences from the matrix-supported deposits described above. Their thicknesses vary from 0.5 cm to 27 cm and the thickest deposits are located between 300 and 1320 cm depth. PSD of the grain-supported deposits are composed of three modes: 450–700 μm, 50–100 μm and 5–8 μm (Fig. 2C). Facies f4 and f2 are characterized by the unique presence of the coarsest and smallest modes, respectively. Calcium content is higher in f4 facies (Fig. 2C).

Laminated deposits

The laminae couplets (<5 mm) are characterized by alternations of dark gray, coarse-grained laminae and white silty clay laminae. PSDs of laminated sediments present the modes 5–8 μm, 50–100 μm and sometimes 450–700 μm, such as in grain-supported deposits. Calcium content is higher in the coarse-grained dark lamina (Fig. 2C). The white silty clay laminae are similar to facies f2 of grain-supported deposits (Fig. 2C).

Age–depth model

The transformation of our flood frequency data set is very sensitive to an age–depth model relationship. Because sedimentary beds thicker than 5 mm represent instantaneous deposits, they were removed from the sediment record when constructing the age–depth model (Fig. 3). Four radiocarbon dates were rejected (Fig. 3), three being obviously too old, probably due to reworked material from a peat deposit being eroded by one of the tributaries (Figs. 1B and C). A contamination of the wood sample during the sampling process may explain the date that is too young. The preliminary age model built using the remaining radiocarbon dates reveals an important increase of sedimentation rate around AD 50–300, implying very high atmospheric lead supplies (36 mg/m^2/a, Fig. 3) during this period when compared to the 20th century maximum of contamination (38 mg/m^2/a, Fig. 3; 32 mg/m^2/a, in Arnaud et al., 2004). This result suggests a local rather than a distant source of lead contamination (Monna et al., 2004). Our previous age–depth model (Giguet-Covex et al., 2011), constructed using the MCAgeDepth software (Higuera et al., 2009), gave a Roman lead pollution slightly too old (130 BC) relative to the conquest of the Upper Arve valley by Romans, between 121 and 61 BC. Therefore, in the present study, we use the "CLAM" program (Blaauw, 2010) allowing integrating chronostratigraphical markers into the age–depth model. The start of Roman lead pollution was assigned an age of 50 BC, just after the settlement of Romans in the Valley, while the lead peak associated with the oil crisis was assigned an AD 1973–74 age. Gravity-reworked sediment deposits associated with earthquakes (see below; Arnaud et al., 2002; Beck, 2009) in AD 1755 (Brigg seism), AD 1817 (Chamonix), AD 1855 (Visp) and AD 1905 (Emosson) (Arnaud et al., 2002) were also taken into account to establish the age–depth model.

Interpretation

Lithology

Matrix-supported sediment deposits

The characteristics of this type of deposit (high sorting values and absence of a clayey layer at the top) suggest that the energy for the

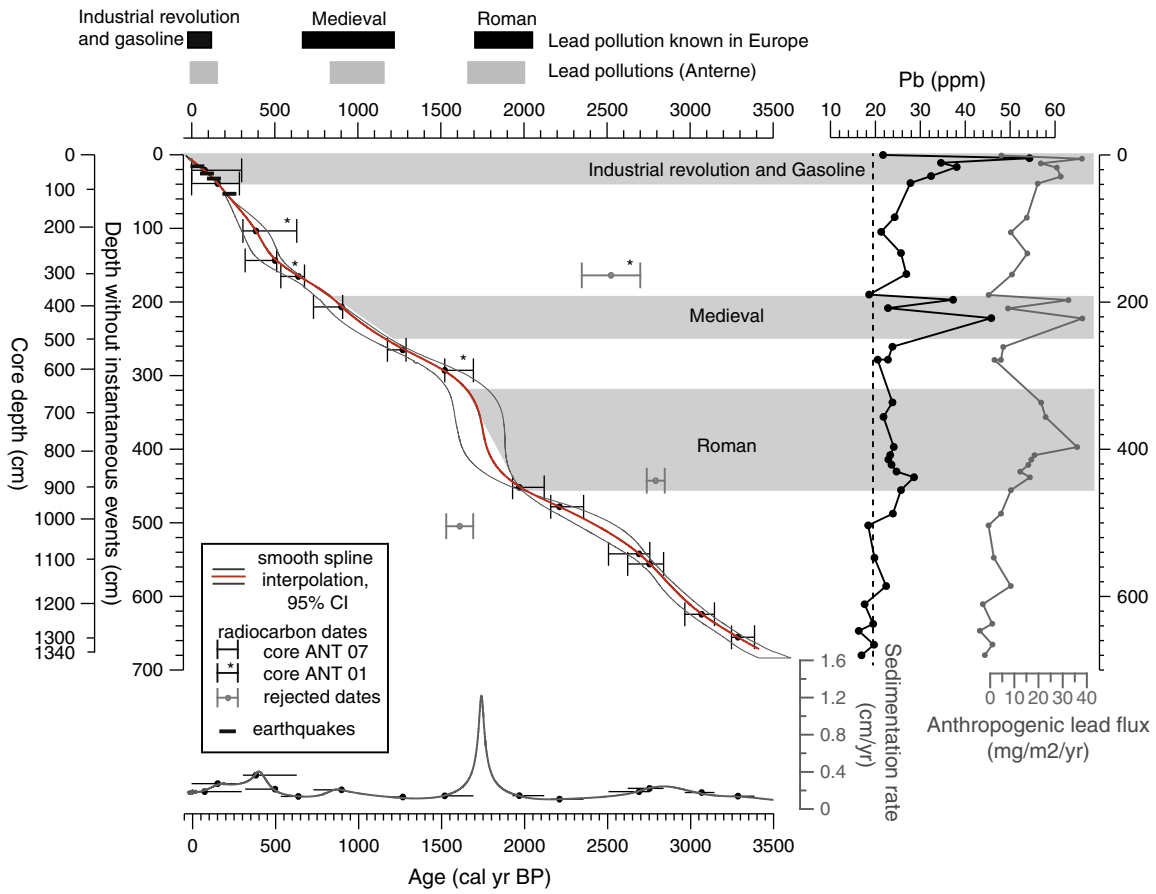

Figure 3. Age–depth model (smooth spline interpolation) obtained from radiocarbon dates, lead pollution during Roman period and the use of leaded gasoline (Giguet-Covex et al., 2011), and earthquakes (Arnaud et al., 2002). Lead concentration and anthropogenic fluxes are presented as records of lead pollutions. The dashed line corresponds to the mean concentration of pre-anthropogenic samples. The sedimentation rate, calculated only taking into account laminated sediments, is also presented with date uncertainties.

transport is provided by the sediment weight. According to the classification of Mulder and Cochonat (1996), this type of deposit may be triggered by a liquefied or a fluidized flow of reworked sediment. Consequently, they were associated with gravity-reworked sediments due to slope failure of the delta foreset (Arnaud et al., 2002; Beck, 2009). Seismic activity seems to be the best explanation for the initiation of these collapses. Four gravity-reworked sediment deposits were associated with high magnitude historically known earthquakes (>7 MSK on the Medvedev–Sponheuer–Karnik seismic intensity scale) (Arnaud et al., 2002) which were used as chronostratigraphical markers in this study. The presence of these deposits mainly after 50 BC, during a period when the sedimentation rates became higher, shows that the delta reached then a critical morphology making it more sensitive to seismic destabilization (Strasser et al., 2007; Beck, 2009).

Grain-supported sediment deposits

The well-sorted base (f4) for these deposits suggests that sediments were transported by a water current (Mulder and Alexander, 2001). Grain-supported sediment deposits were thus interpreted as the result of hyperpycnal turbidity current triggered by floods in the catchment (Arnaud et al., 2002). In such a case, there is a direct link between current velocity and grain size of sediment transported (Pidwirny, 2008). Past and ongoing catchment-scale monitoring of sediment transfer processes confirm the assumption of flood-triggered deposits and show that sediment transport to the lake mainly occurs during rainfall events and not during the seasonal snowmelt (Enters et al., 2009).

Laminated deposits

Long-term monitoring of sediment transfer to the lake showed that the deposition of laminated sediments is also triggered by precipitation events (Enters et al., 2009). Moreover, these monitoring efforts did not indicate any substantial contribution of snowmelt upon sediment transfer within the catchment nor into the lake. The rate of snowmelt probably is not high enough to generate sufficient stream power necessary for the erosion and transportation of particles. Laminations at Lake Anterne do not reflect a seasonal sedimentation pattern but rather individual flood deposits<5 mm triggered by precipitation events as the grain-supported sediment deposits. Coarser sediments composing the dark gray laminae would represent the maximum stream power reached during the event (Cockburn and Lamoureux, 2008). These laminae are deposited in the bottom of the lake through hyperpycnal turbidity currents (Mulder and Alexander, 2001). Light-colored laminae, made of clay and fine silt, reflect the settling of fine sediments when the velocity of inflows decreases. Units representing fine-texture laminae are not necessarily associated with sedimentation below an ice cover in winter.

Indicator of flood intensity

Particle-size distributions of the laminated facies show at several depths the presence of the coarsest mode (450–700 μm), which is also observed in most (87%) of the grain-supported sediment deposits (Figs. 2C and 4). Some flood deposits from the laminated facies have thus been triggered by precipitation events at least as intense as the ones responsible for some thicker flood deposits (grain-supported

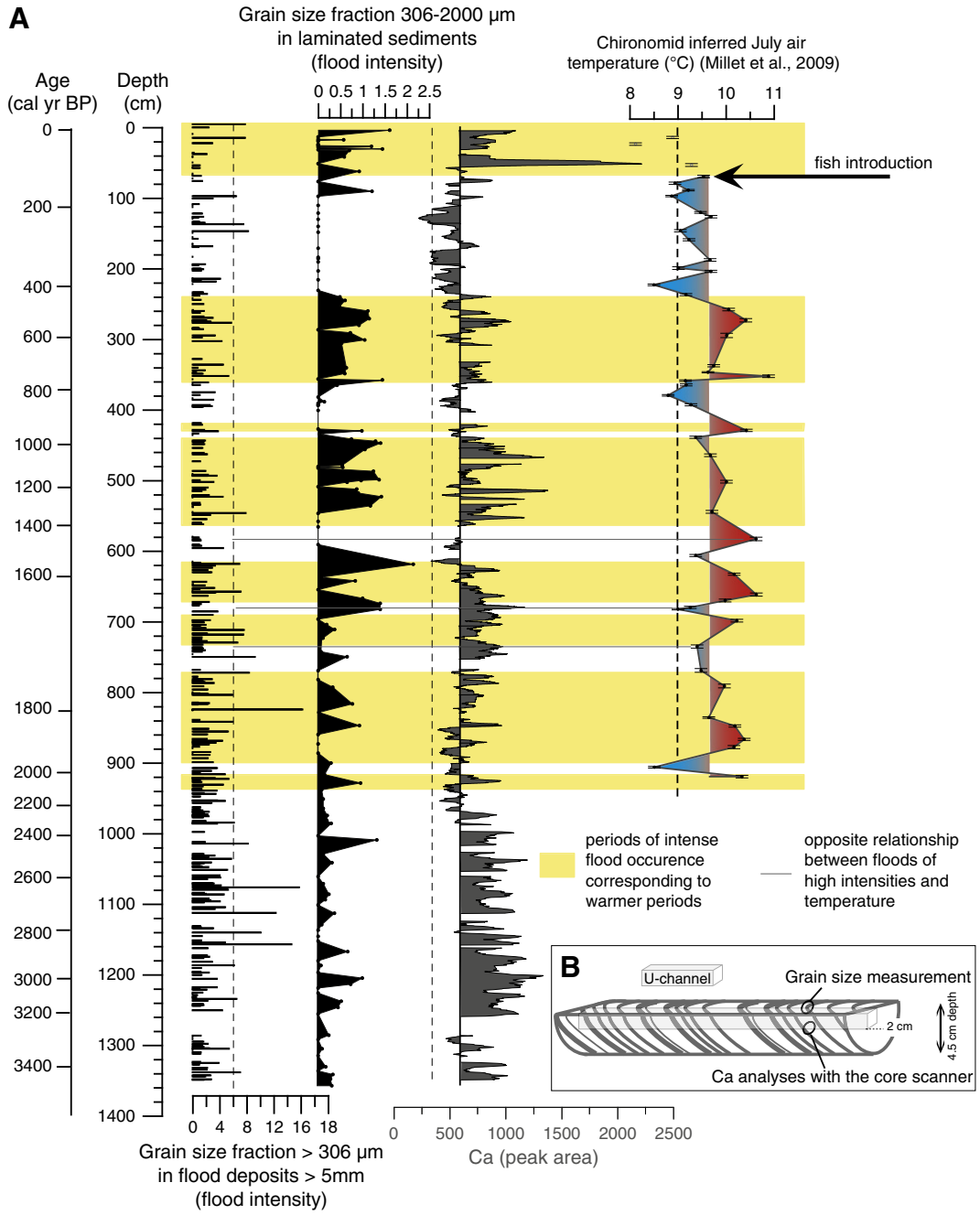

Figure 4. Comparison between the chironomid-inferred July air temperature (°C) (Millet et al., 2009), grain-size fraction 306–2000 µm from laminated sediments and thick flood deposits, and the calcium content (running average at 5 cm) in laminated sediments. Yellow areas correspond to periods of extreme flood occurrence corresponding to warmer temperatures. Gray lines underline periods with opposite relationship.

sediment deposits). Therefore, the thickness of flood deposits is not a reliable indicator for flood intensity in our system. The duration of precipitation events as well as the availability of easily erodible material in the catchment may also have influenced the flood-deposit thickness signal (Blass et al., 2003; Bøe et al., 2006). As a consequence, the fraction of particles coarser than 306 µm in laminated sediments (<5 mm-thick doublets) as well as in the facies 4 of grain-supported sediment deposits (>5 mm grain-supported deposits) was chosen as an indicator of flood intensity.

High-temporal resolution indicator of flood intensity

Because calcium is prevalent in the coarsest facies of laminated and grain-supported thick sediment deposits (dark gray lamina and facies 4, respectively) (Fig. 2C), the calcium record in laminated sediments can be used as a continuous high-resolution proxy of flood intensity in this part of the core. However, calcium content, resampled with the same discontinuous sampling as for grain-size measurements, matches only moderately well with the coarsest fraction (>306 µm) measured in laminated sediments ($n=84$, $r=0.57$, $p<6.10^{-7}$) in the upper 9.4 m (Fig. 4A). We attribute this moderate correlation to sampling-triggered systematic bias related to sediment deformations, linked to piston coring. Furthermore, grain-size measurements were made on samples taken from the core surface, while calcium content was analyzed with the core scanner on the U-channel surface. As shown on Figure 4B, at the same depth, laminated sediments analyzed for grain size and calcium are not the same. Therefore, we cannot perfectly compare both methods.

Furthermore, there is also a little calcium in other facies (Fig. 2C). Thus the absence of coarse particles (particles > 306 μm = 0%) can correspond to different calcium values (between about 270 and 590), which decreases the correlation coefficient between calcium content and the coarsest fraction. Below 9.4 m depth (360 BC), the relationship disappears, which suggests a change in sediment source.

Flood frequency and intensity

Flood frequency signals present variations at both low and high frequencies. Over the last 3.5 ka, two long-lasting periods of 500 and 790 yr of high flood frequency are indicated by laminated doublets < 5 mm and by thick flood deposits > 5 mm (Fig. 5, period A, AD 1380–1880; and period E, 350 BC–AD 440). They correspond to the Little Ice Age (LIA) and the end of Iron Age followed by the Roman Climatic Optimum (RCO), respectively. The high flood frequencies of these two periods are associated with rather different climatic conditions in the Alps (e.g., Holzhauser et al., 2005; Büntgen et al., 2011). Six shorter periods (between 90 and 250 yr) of high flood frequency are also recorded by thin and/or thick flood deposits (Fig. 5). Their ages of occurrence are (b) AD 950–1160, (c) AD 760–850, (d) AD 630–730, (f) 800–550 BC, (g) 1200–1110 BC and (h) 1460–1320 BC (Fig. 5). In spite of some discrepancies, probably linked to dating, seven of these eight phases correspond to wetter periods in the Alps. These wetter periods are mainly characterized by higher lake levels in the Jura and Prealpine mountains (Magny, 2004) and also by advances of the Aletsch glacier advances in the Swiss Alps (Holzhauser et al., 2005) and by Rhone detrital inputs in Lake Le Bourget (Arnaud et al., 2005; Jacob et al., 2009; Debret et al., 2010) (Fig. 5). At least for the last 1255 yr, these periods of high flood frequency tend to associate with cold summers (Büntgen et al., 2006; Fig. 5). Cold climatic conditions seem thus to favor the generation of flood deposits in Lake Anterne.

To investigate the relationship between the occurrence of floods of high intensity and temperature, proxies of flood intensity discussed above (grain size of grain-supported sediment deposits and of laminated sediments and Ca) were compared with previously published chironomid-inferred July air temperatures at Lake Anterne (Millet et al., 2009; Fig. 4A). It is important to note that this method of temperature reconstruction failed for the last hundred years, corresponding to the global warming, due to fish introduction (Millet et al., 2009, Fig. 3A). This approach allowed comparison of proxy data independently of potential discrepancies in the age-model. Although the resolution of the temperature record is lower compared to other proxy data, we observe that floods of higher energy generally occur during periods of warmer temperatures (Fig. 4A). This relationship is well-marked between 0 and 540 cm (AD 690–2007), while below this depth it becomes less clear. This is due to three exceptional samples for which the July temperature presents an opposite relationship with the flood intensity (gray lines, Fig. 4A). This trend of intense precipitation events mainly occurring during warmer climatic conditions is also confirmed by comparison between the calcium content and the tree-ring-based temperature reconstruction in the Swiss and Austrian Alps (Büntgen et al., 2006; Fig. 5). Both curves present very similar trends.

Discussion

Flood-frequency record: climatic control

Conceptually, climatic changes can influence the flood frequency through different factors affecting the sediment mobilization, transport and availability. These factors are: (i) the summer/autumn precipitation, which directly controls the sediment mobilization and transport; (i) the soil stability, which modifies the catchment sensitivity to erosion processes; and (iii) the length of lake ice-free and of catchment snow-covered periods. The soil stability is partly linked to climatic changes through the vegetation cover: warm conditions favor vegetation development and consequently soil stability. On the contrary, cold conditions decrease the soil stability, which increases the sediment availability and makes easier the sediment mobilization during precipitation events. The length of lake ice-free and of catchment snow-cover influence the duration of potential flood record. During warm periods, the longer ice-free lake and the shorter snow-cover periods increase the probability to have floods recorded in lake sedimentation.

In case of Lake Anterne, the highest flood frequencies are observed during cold periods (Fig. 5). This implies that there is no positive correlation between the duration of ice/snow free period and the probability of flood occurrence. Wet and cold conditions, through the rise of rainfall and the reduced soil stability, respectively, more likely explain the record of high flood frequencies. Nonetheless, given the good relationship between high flood frequency and wet periods known in the region (Fig. 5), summer/autumn precipitation events are considered as the main factor driving our flood-frequency signal. Changes in characteristics of vegetation and soil cover probably serve mainly to amplify the flood-frequency signal.

Flood frequency record: land-use effects

Over the last 3.5 ka, one period contradicts the climatic interpretation of our proxies. The period E between 350 BC and AD 440 is characterized by high flood frequencies during a climate that generally was relatively dry and probably warm. A brief departure from dryness occurred between AD 140 and AD 250, when a higher lake level in Jura and Prealpine Massifs increased flooding episodes in Bernese Alps and a small advance of the Aletsch Glacier all occurred (Fig. 5; Magny, 2004; Holzhauser et al., 2005; Schulte et al., 2009, respectively). Nevertheless, the high flood frequency recorded in Lake Anterne during the overall period E cannot be related only to climatic conditions but more probably to human land use. The combination of anthropogenic and climatic effects is hypothesized as responsible for the very high flood frequency recorded between AD 140 and AD 250. Increased presence of grazing herds probably reduced the efficiency of rainfall infiltration due to soil compaction that, in turn, accelerated surface runoff and attacked the protecting herb mat of the soil, leading to its destabilization. Moreover, sediment susceptibility to mobilization is enhanced by clearings and/or fire management for pasture maintenance.

In the Austrian and Swiss Alps, Iron Age (800–60 BC) and Roman periods (60 BC–AD 440) are well known for deforestations and/or grazing activities at high altitude (Schmidt et al., 2002; Heiri and Lotter, 2003; Heiri et al., 2003; Schmidt et al., 2007). Furthermore, a recent palynological investigation of a peat deposit in the vicinity of the study site shows an increase of clearings and pastoral activities during the Roman Period, with a drastic decline of *Alnus viridis* (green alder) and an increase of *Plantago* (plantain) pollen (David, 2010). Despite an intensive archaeological field campaign in 2008 and 2009, only two dwelling remnants were discovered in the catchment of the lake (Rey, 2009, 2010). Charcoal taken in one of these structures at two different stratigraphic positions was dated by ^{14}C (Table 1; Fig. 5). The deepest sample was dated to 385–205 BC (2230 ± 30 ^{14}C yr BP) and the uppermost one to AD 85–245 (1835 ± 30 ^{14}C yr BP). Furthermore, shards of Gallo-Roman ceramic were found. These results denote human presence in the catchment area at least during the end of Iron Age and the Roman Period. This sparse evidence support the hypothesis of a possible anthropogenic impact on vegetation capable of causing soil destabilization and increased surface runoff that could have contributed to the flood-frequency signal.

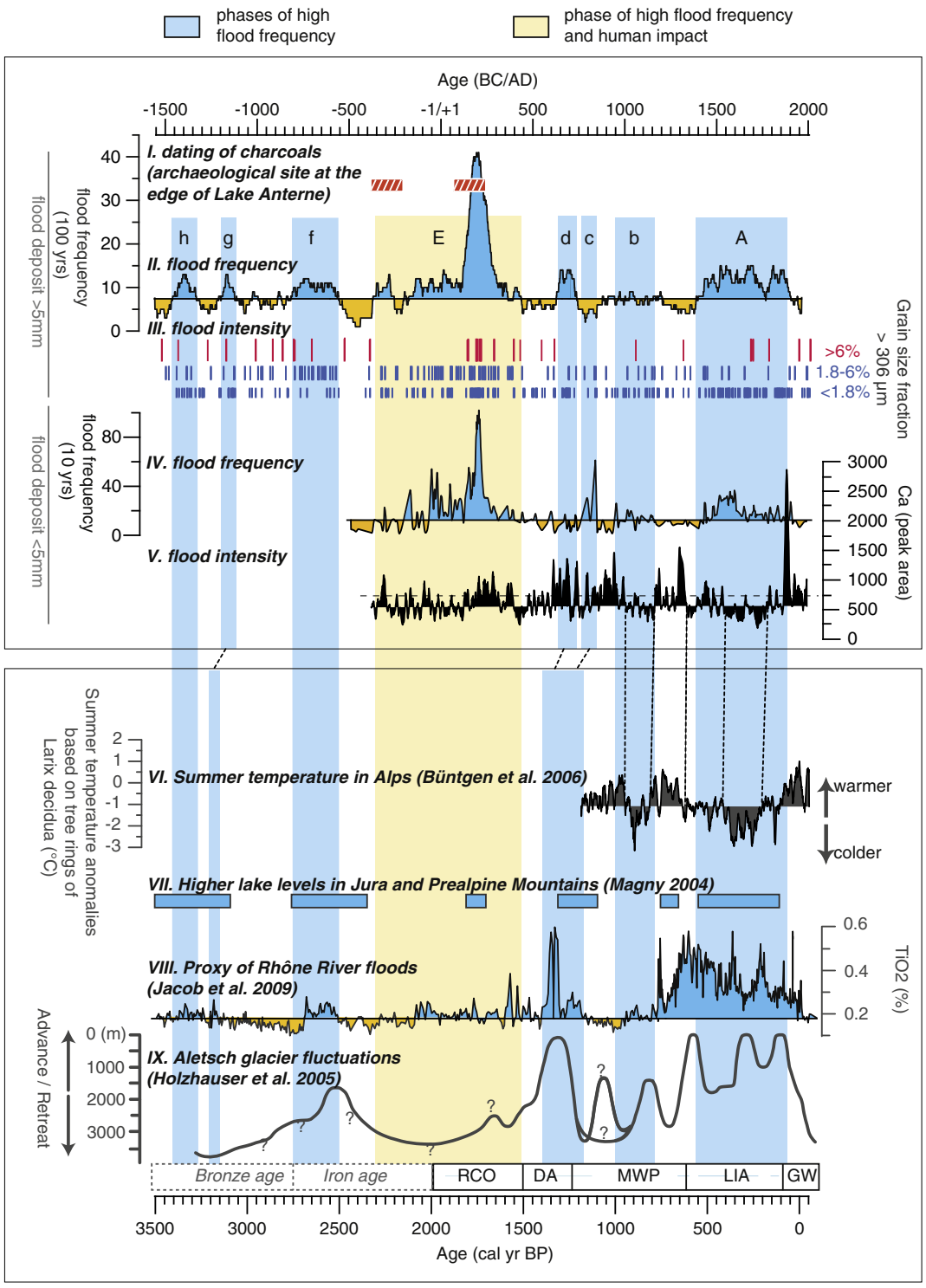

Figure 5. Comparison between flood frequency and intensity and regional climatic records. Rectangles (I) represent the ^{14}C dating of charcoal found in the archaeological site at the edge of Lake Anterne. Curves II and IV correspond to the flood frequencies of thick and thin flood deposits respectively. Records III and V present the evolution of flood intensity: the fraction 306–2000 µm and the calcium content (running mean over a 10-yr interval) for thick and thin flood deposits, respectively. These data are compared to the summer temperature reconstruction (Curve VI) (Büntgen et al., 2006) and the regional hydrological activity: (VII) high lake level in Jura Mountains (Magny, 2004), (VIII) Rhône River floods recorded in Lake Le Bourget sediments (Jacob et al., 2009) and (IX) Aletsch Glacier fluctuations (Holzhauser et al., 2005). Blue rectangles correspond to phases of high flood frequencies and the orange rectangle to period of high flood frequency, linked to human activities (also associated with the dating of archaeological site).

Intensity versus frequency of floods

Our study shows that flood frequency increases during cold periods. However, floods of high intensity occur preferentially during warm periods. The positive relationship between summer temperature and the occurrence of floods of high intensity is particularly clear in the <5-mm flood-deposit record (i.e., Ca signal; Fig. 5). During the last 1250 yr, periods with summer temperature anomalies around the mean of −1°C, represented by the LIA between AD 1390 and 1530 and later decades between AD 1790 and 1880,

are characterized by both high flood frequencies and floods of high intensity. However, floods were not as frequent and intense as during periods of warm conditions (Fig. 5). This result suggests that mild temperatures, neither very cold nor very warm, are favorable to humid conditions with occasional intense precipitation events.

Over the last 3.5 ka, periods E (350 BC–AD 440), D (AD 630–730), and C (AD 760–850) represent times of both high flood frequency and floods of high intensity. During the dry and probably warm period E, representing the end of Iron Age and the Roman Period, this association of frequency and intensity probably is explained by human activities that have increased the flood frequency. These human activities probably also affected the flood intensity through accelerating surface runoff and increasing associated stream velocities. However, the relatively good relationship with the summer temperature for the last 1250 yr (Fig. 5) suggests that human activities are not the main factor controlling the occurrence of high-intensity floods during this period. Periods C and D of high flood frequencies, only recorded by thin flood deposits and thick flood deposits, respectively, also record floods of high intensity. In these two cases, the presence of both frequent floods and floods of high intensity is not well understood. It would be necessary to have a detailed reconstruction of summer temperatures in the Alps to interpret the interactive environmental patterns during these periods. Likewise, the discrepancy between the records of thin and thick flood frequencies during these periods is not well explained. It could reflect differences in sediment availability in the catchment and/or in precipitation event duration.

Our flood record underlines the complexity of interactions between temperature, precipitation, human activities, and soils and erosion processes. In order to better understand the flood intensity and frequency patterns, flood deposits thicker than 5 mm were classified according to their thickness, depending on flood-event duration, intensity and sediment availability, and the proportion of sediment within the 306–2000 µm particle range. The sediment fractions between size classes were determined from the 50th and 90th percentiles of the dataset. The grain-size limit between the thickness classes corresponds to a separation between two different flood-deposit patterns underlined by a bi-plot: the 95th percentile of particle size distribution vs. the flood deposit thickness (Giguet-Covex et al., 2011). For each class, a probability of flood occurrence, expressed in percent, was calculated for warm and cold periods and for the period of suspected human impact (350 BC–AD 440) (Fig. 6). Flood deposits representing high and low intensity, between 0.5 and 6.3 cm thickness, present contrasting probabilities of occurrence in warm and cold climatic conditions (Fig. 6). This classification confirms that floods of high intensity, which are rare, have a higher probability of occurrence during warm periods. On the

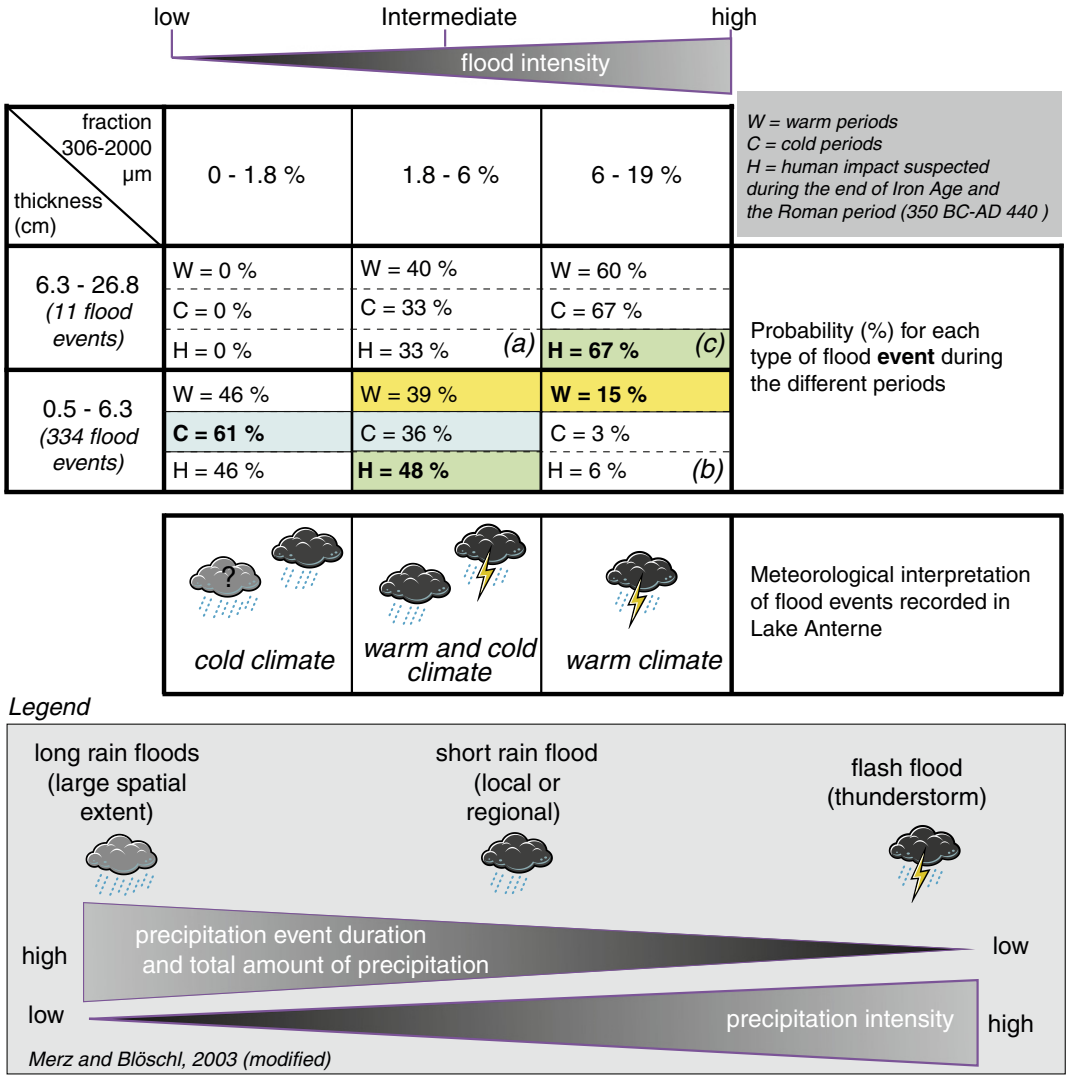

Figure 6. Classification of the flood deposits > 5 mm according to their thickness and coarse particle fraction represented by the proportion of particles coarser than 306 µm. The values correspond to the probability (%) to have the different types of thick floods. An association with the different types of precipitation events (according to Merz and Blöschl, 2003) is also presented.

contrary, floods of lower intensity have a high chance to occur, mostly in cold periods. For the few relatively thick flood deposits, there is no very clear climatic pattern. However, we note that thick floods of low intensity do not exist, which underlines the role of runoff intensity in processes triggering these flood deposits. During periods of strong human activities and characterized by warm and dry climate, the thickest flood deposits representing intermediate intensities (Fig. 6, box a) and the thinnest flood deposits representing high intensities (Fig. 6, box b) are less numerous than in warm periods. However, the thickest flood deposits of high intensity (Fig. 6, box c) are more numerous. These observations confirm the importance of sediment availability, soil stability and runoff intensity on flood generation during times of human impact.

Our results thus imply the coexistence of two climate-dependent flood responses to environmental change on the same site and they show the complex response of erosion patterns to climatic changes in mountain areas. Precipitation events associated with the different flood types recorded in Lake Anterne, and mainly based on flood intensity, are proposed in Figure 6 (Merz and Blöschl, 2003). According to this model, floods of high intensity correspond to flash floods. These floods are generated by extreme rainfall triggered by convective storms only occurring in summer (June, July, August; Merz and Blöschl, 2003). The higher probability of a small catchment, such as Anterne, to encounter floods linked to severe convective storms (Schmocker-Fackel and Naef, 2010), explains the sensitivity of our record to these events and their absence in sediments of Lake Le Bourget. Floods of high frequency but low intensity, rather recorded in cold periods in Lake Anterne, are associated with floods of large spatial extent. Generation of long-duration rain floods in Anterne catchment is probably promoted in case of human pressure, making easier for sediment mobilization. The model built in our small mountain area thus suggests that warm periods are more favorable to the occurrence of thunderstorms. Consequently, they are expected to increase in the context of global warming. This assumption is supported by a simulation showing an increase of severe convective storms over Europe (Sander and Dotzek, 2010). A general decrease of annual average precipitation and increase of extreme precipitation events is also noted for some years and is predicted for the future in Western Europe in the context of global warming (Easterling, et al., 2000; Christensen and Christensen, 2003; Brunetti, et al., 2004; Fuhrer et al., 2006). All these studies suggest that, on average, drier conditions are associated with a higher probability of extreme precipitation events during anomalously warm periods, a conclusion that is supported by our results for the last 3.5 ka.

Studies in Switzerland and Italy suggested that changes in flood and precipitation patterns might be triggered by modifications of atmospheric circulation (Brunetti, et al., 2004; Schmocker-Fackel and Naef, 2010). Such relationships cannot be determined from our data. However, future meteorological studies based on models or historical data, as well as intensive on-site monitoring, will improve understandings of the complex relationships between changes in flood patterns and atmospheric circulation regimes.

Conclusion

Detailed sedimentary and geochemical characterization of late Holocene deposits in an alpine lake provides a long-term record of flood event frequency and intensity. This study documents temporal changes in floods in the northwest European Alps since 3.5 ka. Results show that floods are more frequent during relatively cool and wet periods, although extreme floods are more frequent when warmer summer climate conditions prevail. Although the origin of this pattern is not completely understood at present, these results constitute an important source of information to better understand past and future changes of hydrological patterns and future natural hazard management in alpine catchments in a context of global warming.

Our results also suggest that anthropogenic activities such as clearing and grazing contributed to the complexity of flood signals through impacts on vegetation cover and soil properties. Effects of these activities were mainly observed on flood frequency during the end of the Iron Age and during the Roman Period. Human land-use activities probably increased the sensitivity of the sediment record to floods triggered by precipitation events of low intensity.

Acknowledgments

Analytical results were acquired in the framework of the scientific programs Aphrodyte and Pygmalion, founded by the CNRS program Eclipse and the French National Research Agency (ANR BLAN07-2_204489), respectively. Radiocarbon dating was performed by the national facility LM14C in the framework of the INSU ARTEMIS call-for-proposal. Grain size measurements were performed thanks to the ASTRE platform, a facility of the University of Savoie. We thank guards of the Sixt-Passy Natural Reserve for their assistance during fieldwork and ASTERS, the manager of Haute Savoie natural reserves, for constant support.

References

Allen, M.R., Ingram, W.J., 2002. Constraints on future changes in climate and the hydrological cycle. Nature 419, 224–232.
Arnaud, F., Lignier, V., Revel, M., Desmet, M., Beck, C., Pourchet, M., Charlet, A., Trentesaux, A., Tribovillard, N., 2002. Flood and earthquake disturbance of 210Pb geochronology (Lake Anterne, North French Alps). Terra Nova 14–4, 225–232.
Arnaud, F., Revel-Rolland, M., Bosch, D., Winiarski, T., Chapron, E., Desmet, M., Tribovillard, N., Givelet, N., 2004. A reliable 300 years-long history of lead contamination in Northern French Alps from distant lake sediment records. Journal of Environmental Monitoring 6–5, 448–456.
Arnaud, F., Revel-Rolland, M., Chapron, E., Desmet, M., Tribovillard, N., 2005. 7200 years of Rhône river flooding activity recorded in Lake Le Bourget: a high resolution sediment record of NW Alps hydrology. The Holocene 15–3, 420–428.
Arnaud, F., Serralongue, J., Winiarski, T., Desmet, M., Paterne, M., 2006. Pollution au plomb dans la Savoie antique (II–IIIe s ap J-C) en relation avec une installation métallurgique de la cité de Vienne. Comptes Rendus — Géosciences 338, 244–252.
Beck, C., 2009. Late Quaternary lacustrine paleo-seismic archives in north-western Alps: examples of earthquake-origin assessment of sedimentary disturbances. Earth-Science Reviews 96, 327–344.
Beniston, M., Diaz, H.F., Bradley, R.S., 1997. Climatic change at high elevation sites: an overview. Climatic Change 36, 233–251.
Benito, G., Lang, M., Barriendos, M., Llasat, M.C., Francés, F., Ouarda, T., Thornydcraft, V.R., Enzel, Y., Bardossy, A., Coeur, D., Bobée, B., 2004. Use of systematic, paleoflood and historical data for improvement of flood risk estimation, review of scientific methods. Natural Hazards 3, 623–643.
Blaauw, M., 2010. Methods and code for 'classical' age-modelling of radiocarbon sequences. Quat. Geochronology 5, 512–518.
Blass, A., Anselmetti, F.S., Ariztegui, D., 2003. 60 years of glaciolacustrine sedimentation in Steinsee (Sustenpass, Switzerland) compared with historic events and instrumental meteorological data. Eclogae geol. Helv. 96 Supplement 1, S59–S71.
Bøe, A.G., Dahl, S.O., Lie, Ø., Nesje, A., 2006. Holocene river floods in the upper Glomma catchment, southern Norway: a high-resolution multiproxy record from lacustrine sediments. The Holocene 16, 445–455.
Brunetti, M., Buffoni, L., Mangianti, F., Maugeri, M., Nanni, T., 2004. Temperature, precipitation and extreme events during the last century in Italy. Global and Planetary Change 4, 141–149.
Büntgen, U., Frank, D.C., Nievergelt, D., Esper, J., 2006. Summer temperature variations in the European Alps, A.D. 755–2004. Journal of Climate 19, 5606–5623.
Büntgen, U., Tegel, W., Nicolussi, K., McCormick, M., Frank, D., Trouet, V., Kaplan, J.O., Herzig, F., Heussner, K.-U., Wanner, H., Luterbacher, J., Esper, J., 2011. 2500 years of European climate variability and human susceptibility. Science 331, 578–582. doi:10.1126/science.1197175.
Bussmann, F., Anselmetti, F., 2010. Rosseberg landslide history and flood chronology as recorded in Lake Lauerz sediments (Central Switzerland). Swiss Journal of Geosciences 103, 43–59.
Campbell, C., 1998. Late Holocene Lake sedimentology and climate change in Southern Alberta, Canada. Quaternary Research 49, 96–101.
Christensen, J.H., Christensen, O.B., 2003. Severe summertime flooding in Europe. Nature 421, 805.
Cockburn, J.M.H., Lamoureux, S.F., 2008. Inflow and lake controls on short-term mass accumulation and sedimentary particle size in a High Arctic lake: implications for interpreting varved lacustrine sedimentary records. Journal of Paleolimnology 40, 923–942.
Croudace, I.W., Rindby, A., Rothwell, G., 2006. ITRAX: description and evaluation of a new multi-function X-ray core scanner. In: Rothwell, R.G. (Ed.), New Techniques in Sediment Core Analysis. Publication, Geological Society of London Special, pp. 51–63.

Dapples, F., Lotter, A.F., van Leeuwen, J.F.N., van der Knapp, W.O., Dimitriadis, S., Oswald, D., 2002. Paleolimnological evidence for increased landslide activity due to forest clearing and land-use since 3600 cal BP in the western Swiss Alps. Journal of Paleolimnology 27, 239–248.

David, F., 2010. Expansion of green alder (*Alnus alnobetula* (Ehrh) K.Koch) in the northern French Alps: a palaeoecological point of view. Compte Rendu de l'Académie des sciences, Biologies 333, 424–428. doi:10.1016/j.crvi.2010.01.002.

Debret, M., Chapron, E., Desmet, M., Rolland-Revel, M., Magand, O., Trentesaux, A., Bout-Roumazeille, V., Nomade, J., Arnaud, F., 2010. North western Alps Holocene paleohydrology recorded by flooding activity in Lake Le Bourget. France. Quatern. Sci. Rev. 29, 2185–2200.

Easterling, D.R., Meehl, G.A., Parmesan, C., Changnon, S.A., Karl, T.R., Mearns, L.O., 2000. Climate extremes: observation, modeling, and impacts. Science 289, 2068–2074.

Enters, D., Arnaud, F., Poulenard, J., Giguet-Covex, C., Malet, E., Wilhelm, B., 2009. A Coupled Environmental Monitoring and Lake Sediment Study to Understand Factors Generating Torrential Floods in an Alpine Catchment (Giffre Valley, NW French Alps). EGU Congress, Austria.

Francus, P., Bradley, R.S., Abbott, M.B., Patridge, W., Keimig, F., 2002. Paleoclimate studies of minerogenic sediments using annually resolved textural parameters. Geophysical Research Letters 29, 20 (1998).

Fuhrer, J., Beniston, M., Fischlin, A., Frei, Ch., Goyette, S., Jasper, K., Pfister, Ch., 2006. Climate risks and their impact on agriculture and forests in Switzerland. Climatic Change 79, 79–102.

Frei, C., Christensen, J.H., Déqué, M., Jacob, D., Jones, R.G., Vidale, P.L., 2003. Daily precipitation statistics in regional climate models: evaluation and intercomparison for the European Alps. Journal of Geophysical Research 108 (D3), 4124. doi:10.1029/2002JD002287.

Frei, C., Schöll, R., Fukutome, S., Schmidli, J., Vidale, P.L., 2006. Future change of precipitation extremes in Europe: intercomparison of scenarios from regional climate models. Journal of Geophysical Research 111. doi:10.1029/2005JD005965.

Giguet-Covex, C., Arnaud, F., Poulenard, J., Disnar, J.-R., Delhon, C., Francus, P., David, F., Enters, D., Rey, P.-J., Delannoy, J.-J., 2011. Changes in erosion patterns during the Holocene in a currently treeless subalpine catchment inferred from lake sediment geochemistry (Lake Anterne, 2063 m a.s.l., NW French Alps): the role of climate and human activities. The Holocene 12, 651–665. doi:10.1177/0959683610391320.

Heiri, O., Lotter, A.F., 2003. 9000 years of chironomid assemblage dynamics in an Alpine lake: long-term trends, sensitivity to disturbance, and resilience of the fauna. Journal of Paleolimnology 30, 273–289.

Heiri, O., Wick, L., van Leeuwen, J.F.N., van der Knaap, W.O., Lotter, A.F., 2003. Holocene tree immigration and the chironomid fauna of a small Swiss subalpine lake (Hinterburgsee, 1515 m asl). Paleogeography, Paleoclimatology, Paleoecology 189, 35–53.

Higuera, P.E., Brubaker, L.B., Anderson, P.M., Hu, F.S., Brown, T.A., 2009. Vegetation mediated the impacts of postglacial climate change on fire regimes in the South central Brooks Range, Alaska. Ecological Monographs 79, 201–219.

Holzhauser, H., Magny, M., Zumbühl, H.J., 2005. Glacier and lake-level variations in west-central Europe over the last 3500 years. The Holocene 15, 789–801.

Jacob, J., Disnar, J.-R., Arnaud, F., Gauthier, E., Billaud, Y., Chapron, E., Bardoux, G., 2009. Impacts of new agricultural practices on soil erosion during the Bronze Age in the French Prealps. The Holocene 19 (2), 241–249.

Lanci, L., Hirt, A.M., Lotter, A.F., Sturm, M., 2001. A record of Holocene climate in the mineral magnetic record of Alpine lakes: Sägistalsee and Hinterburgsee. Earth and Planetary Science Letters 188, 29–44.

Leeman, A., Niessen, F., 1994. Holocene glacial activity and climatic variations in the Swiss Alps: reconstructing a continuous record from proglacial lake sediments. The Holocene 4, 259–268.

Magny, M., 2004. Holocene climate variability as reflected by mid-European lake-level fluctuations and its probable impact on prehistoric human settlements. Quaternary International 113, 65–79.

Merz, R., Blöschl, G., 2003. Regional flood risk_what are the driving processes? Water resources systems-hydrological risk, management and development (proceedings of symposium HS02b held during IUGG2003 at Sapporo). IAHS 281, 49–58.

Millet, L., Arnaud, F., Heiri, O., Magny, M., Verneaux, V., Desmet, M., 2009. Late-Holocene summer temperature reconstruction from chironomid assemblages of Lake Anterne, northern French Alps. The Holocene 19 (2), 317–328.

Monna, F., Galop, C., Carozza, L., Tual, M., Beyrie, A., Marembert, F., Chateau, C., Domink, J., Grousset, F.E., 2004. Environmental impact of early Basque mining and smelting recorded in a high ash minerogenic peat deposit. Science of the Total Environment 327, 197–214.

Mulder, T., Cochonat, P., 1996. Classification of offshore mass movements. Journal of Sedimentary Research 66, 43–57.

Mulder, T., Alexander, J., 2001. The physical character of subaqueous sedimentary density flows and their deposits. Sedimentology 48, 269–299.

Nesje, A., Olaf Dahl, S., Matthews, J.A., Berrisford, M.S., 2001. A 4500-yr record of river floods obtained from a sediment core in Lake Atnsjøen, eastern Norway. Journal of Paleolimnology 25, 329–342.

Palmer, T.N., Räisänen, J., 2002. Quantifying the risk of extreme seasonal precipitation events in a changing climate. Nature 415, 512–514.

Parris, A.S., Bierman, P.R., Noren, A.J., Prins, M.A., Lini, A., 2009. Holocene paleostorms identified by particle size signatures in lake sediments from the northeastern United States. Journal of Paleolimnology. doi:10.1007/s10933-009-9311-1.

Pidwirny, Michael. 2008. Soil erosion and deposition. Encyclopedia of Earth, Editor Cutler J. Cleveland. <http://www.eoearth.org/article/Soil_erosion_and_deposition>. Topic Editor, Draggan, Sidney. Environmental Information Coalition (EIC) of the National Council for Science and the Environment (NCSE), Washington D.C., USA.

R Development Core Team, 2011. R: A Language and Environment for Statistical Computing. R Foundation for Statistical Computing, Vienna, Austria3-900051-07-0 http://www.R-project.org/.

Rebetez, M., Lugon, R., Baeriswyl, P.A., 1997. Climatic change and debris flow in high mountain regions: the case study of the Ritigraben torrent (Swiss Alps). Climatic Change 36, 371–389.

Reimer, P.J., Baillie, M.G.L., Bard, E., Bayliss, A., Beck, J.W., Blackwell, P.G., Bronk Ramsey, C., Buck, C.E., Burr, G.S., Edwards, R.L., Friedrich, M., Grootes, P.M., Guilderson, T.P., Hajdas, I., Heaton, T.J., Hogg, A.G., Hughen, K.A., Kaiser, K.F., Kromer, B., McCormac, F.G., Manning, S.W., Reimer, R.W., Richards, D.A., Southon, J.R., Talamo, S., Turney, C.S.M., van der Plicht, J., Weyhenmeyer, C.E., 2009. IntCal09 and Marine09 radiocarbon age calibration curves, last 50,000 years cal BP. Radiocarbon 51, 1111–1150.

Rey, P.J., 2009. Premières occupations de la montagne sur les versants du col d'Anterne (2257 mètres). Bilan scientifiques de la région Rhône Alpes 2008, Ministère de la culture et de la communication, pp. 205–207.

Rey, P.J., 2010. Passy-Servoz : les premières occupations des versants du col d'Anterne. Bilan scientifiques de la région Rhône Alpes 2009, Ministère de la culture et de la communication, pp. 198–200.

Rico, M., Benito, G., Barnolas, A., 2001. Combined paleoflood and rainfall–runoff assessment of mountain floods (Spanish Pyrenees). Journal of Hydrology 245, 59–72.

Sander, J., Dotzek, N., 2010. The impact of climate change on severe convective storms over Europe. EMS Annual Meeting Abstracts 7, 532.

Schmidt, R., Koining, K.A., Thompson, R., Kamenik, C., 2002. A multi proxy core study of the last 7000 years of climate and alpine land-use impacts on an Austrian mountain lake (Unter Landschitzsee, Niedere Tauern). Palaeogeography, Palaeoclimatology, Palaeoecology 187, 101–120.

Schmidt, R., Kamenik, C., Roth, M., 2007. Siliceous algae-based seasonal temperature inference and indicator pollen tracking ca. 4,000 years of climate/land use dependency in the southern Austrian Alps. Journal of Paleolimnology 38, 541–554.

Schmocker-Fackel, P., Naef, F., 2010. More frequent flooding in Switzerland since 1850. Journal of Hydrology 381, 1–8.

Schulte, L., Veit, H., Burjachs, F., Julià, R., 2009. Lütschine fan delta response to climate variability and land use in the Bernese Alps during the last 2400 years. Geomorphology 108, 107–121.

Strasser, M., Stegmann, S., Bussmann, F., Anselmetti, F.S., Rick, B., Kopf, A., 2007. Quantifying subaqueous slope stability during seismic shaking: Lake Lucerne as model for ocean margins. Marine Geology 240, 77–97.

Trask, P.D., 1930. Mechanical analysis of sediments by centrifuge. Economic Geology 25, 581–599.

Trenberth, K.E., 1999. Conceptual framework for changes of extremes of the hydrological cycle with climate change. Climatic Change 42, 327–339.